JOURNAL OF NATURAL PRODUCTS

Article

pubs.acs.org/jnp

Acridone Alkaloids from *Glycosmis chlorosperma* as DYRK1A Inhibitors

Mehdi A. Beniddir,[†] Erell Le Borgne,[†] Bogdan I. Iorga,[†] Nadège Loaëc,[‡,§] Olivier Lozach,[‡] Laurent Meijer,[‡,§] Khalijah Awang,[⊥] and Marc Litaudon*[,†]

[†]Centre de Recherche de Gif, Institut de Chimie des Substances Naturelles, CNRS, LabEx CEBA, 1, Avenue de la Terrasse, 91198 Gif-sur-Yvette Cedex, France

[‡]Protein Phosphorylation & Human Disease group, CNRS, Station Biologique de Roscoff, BP 74, 29682 Roscoff, France

[§]ManRos Therapeutics, Centre de Perharidy, 29680 Roscoff, France

[⊥]Department of Chemistry, University Malaya, 59100 Kuala Lumpur, Malaysia

Supporting Information

ABSTRACT: Two new acridone alkaloids, chlorospermines A and B (**1** and **2**), were isolated from the stem bark of *Glycosmis chlorosperma*, together with the known atalaphyllidine (**3**) and acrifoline (**4**), by means of bioguided isolation using an in vitro enzyme assay against DYRK1A. Acrifoline (**4**) and to a lesser extent chlorospermine B (**2**) and atalaphyllidine (**3**) showed significant inhibiting activity on DYRK1A with IC_{50}'s of 0.075, 5.7, and 2.2 μM, respectively. Their selectivity profile was evaluated against a panel of various kinases, and molecular docking calculations provided structural details for the interaction between these compounds and DYRK1A.

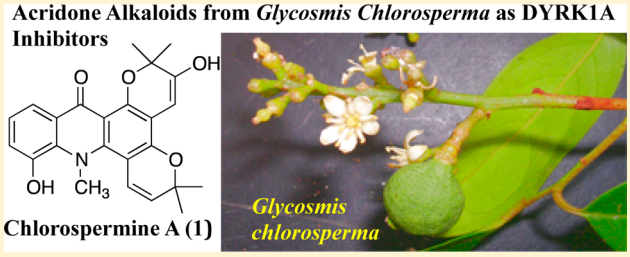

Newly developed tools, such as synthetic small-molecule inhibitors, genetic modulation, RNAi technology, and bioinformatics, revealed that protein kinases are involved in almost all human diseases, including cancer, diabetes, cardiovascular diseases, developmental disease, neurological disease, and infectious disease.[1] Dual-specificity tyrosine phosphorylation-regulated kinase 1A (DYRK1A) is a protein kinase with diverse functions and is implicated in neuronal development and adult brain physiology. Higher than normal levels of DYRK1A are associated with the pathology of neurodegenerative diseases and have been implicated in some neurobiological alterations of Down syndrome, such as mental retardation.[2] In this context and in continuation of our biological screening program of plant extracts from tropical regions for the discovery of bioactive natural product kinase inhibitors,[3a,b] a total of 702 ethyl acetate extracts previously filtered on polyamide cartridges and 18 alkaloid extracts obtained from different parts of plants were screened for their inhibitory activity against DYRK1A, leading to the selection of *Glycosmis chlorosperma* (Blume) Spreng,[4] (Rutaceae) for this investigation.

Glycosmis (Rutaceae) is a genus of approximately 50 species of glabrous shrub, distributed in warm and temperate regions of the world including 15 species in Malaysia.[5] Previous phytochemical reports indicated that the genus *Glycosmis* is a rich source of various classes of compounds such as flavonoids,[6a,b] acridone-,[7a−d] carbazole-,[8a−c] quinolone-,[9] and quinazoline-alkaloids,[10] and sulfur-containing amides.[11a−d]

The present report describes the bioassay-guided isolation, structural elucidation, and DYRK1A-inhibiting activity of four acridone alkaloids (**1**−**4**), including the new compounds **1** and **2**, from the dried stem bark of *G. chlorosperma*. The compounds were also tested on the closely related cdc2-like kinase CLK1, and the selectivity profile of the compounds was finally evaluated by including cyclin-dependent kinases 1 and 5 (CDK1 and CDK5), glycogen synthase kinase-3 (GSK3), and casein kinase 1 (CK1).

RESULTS AND DISCUSSION

From the 720 organic extracts tested on DYRK1A, only 11 (eight EtOAc and three alkaloid extracts) showed a significant inhibiting activity ($IC_{50} \leq 10$ μg/mL), of which the EtOAc bark extract of *G. chlorosperma* exhibited the most potent activity, with an IC_{50} value of 0.66 μg/mL (Figure 1). This extract was subjected to C_{18} flash chromatography to afford 12 fractions. The biologically active fraction F6 (IC_{50} 0.23 μg/mL) was further purified using silica gel and C_{18} column chromatographies, leading to the isolation of two new acridone alkaloids, chlorospermines A and B (**1** and **2**), along with the known atalaphyllidine (**3**)[12] and acrifoline (**4**).[7d]

The HRESIMS spectrum of chlorospermine A (**1**) indicated an $[M + H]^+$ ion at m/z 406.1656, which, in conjunction with the ^{13}C NMR spectroscopic data, is consistent with a molecular

Received: October 11, 2013
Published: May 5, 2014

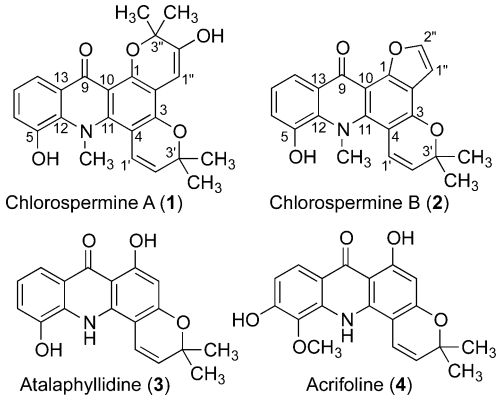

formula of $C_{24}H_{24}NO_5$ (calcd 406.1654), indicating 14 indices of hydrogen deficiency. The UV spectrum exhibited characteristic absorption bands at 275 and 303 nm for an acridone core.[13] The IR spectrum of **1** showed strong absorption bands at 3210 cm^{-1} for hydroxy groups and 1595 cm^{-1} for a carbonyl function. The ^1H NMR data of **1** (Table 1) revealed the presence of two 2,2-dimethylpyran moieties. The first ring showed a set of doublets at δ_H 6.95 and 5.52 for H-1′ and H-2′, respectively, each with a 9.8 Hz coupling constant. The second 2,2-dimethylpyran ring was slightly different, and its ^1H NMR showed the presence of only one singlet at δ_H 6.60 as well as a C-2″ hydroxy group. The four methyl groups of the two pyran rings resonated as two singlets (six protons each) at δ_H 1.52 and 1.70. In addition, the ^1H NMR spectrum showed aromatic resonances for a 1,2,3-trisubstituted benzene ring as well as an *N*-methyl resonance at δ_H 3.75. The ^{13}C and DEPT 135 ^{13}C NMR spectra confirmed the presence of 24 carbons, consisting of five methyl, six sp^2 methine, two sp^3 quaternary, and 11 sp^2 quaternary carbons. The location of the first pyran ring was revealed by the NOESY correlation between H-1′ and the *N*-methyl protons and was confirmed by the HMBC correlations from H-1′ and H-2′ to C-3′ and C-4. The HMBC correlations from H-1″ to C-2″, C-1, and C-2 established the location of the second pyran moiety (Figure 2). Analysis of COSY, HSQC, and HMBC data confirmed the assignment of the entire structure, and the compound was given the trivial name chlorospermine A (**1**).

Table 1. NMR Spectroscopic Data for Chlorospermines A (1) and B (2) in $CDCl_3$

	1		2	
position	δ_H (J in Hz)[a]	δ_C[b]	δ_H (J in Hz)[a]	δ_C[b]
1		153.6		154.2
2		114.2		113.7
3		153.1		152.8
4		106.7		106.5
5		148.3		148.4
6	7.39, br, d (7.2)	120.4	7.07, m	119.0
7	6.97, m	123.6	7.09, t (7.5)	123.4
8	7.79	117.4	7.89, dd (7.5, 1.5)	117.5
9		177.1		177.5
10		107.6		108.2
11		147.1		147.2
12		137.4		137.2
13		126.9		127.7
1′	6.95, d (9.8)	126.9	6.77, d (9.7)	121.8
2′	5.52, d (9.8)	123.8	5.54, d (9.7)	124.1
3′		77.3		77.3
4′	1.52, s	27.2	1.53, s	27.2
5′	1.52, s	27.2	1.53, s	27.2
1″	6.60, s	97.1	6.83, d (1.9)	103.6
2″		162.7	7.68, d (1.9)	144.5
3″		68.8		
4″	1.70, s	28.7		
5″	1.70, s	28.7		
N-CH_3	3.75, s	48.7	3.73, s	48.4

[a]Data recorded at 500 MHz. [b]Data recorded at 125 MHz.

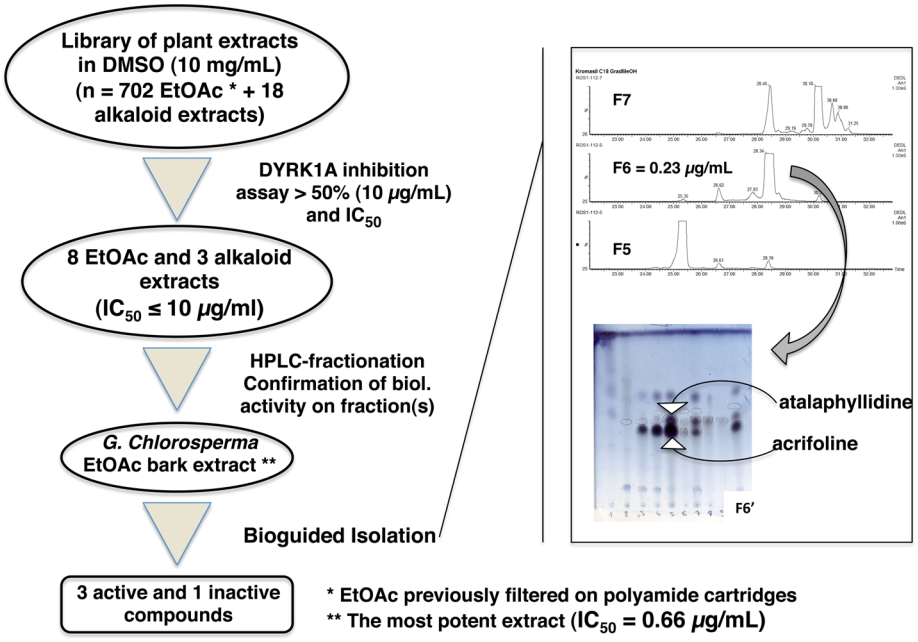

Figure 1. Workflow for the discovery of acridone alkaloids as new DYRK1A inhibitors: HPLC analytical control of fractions F5, F6, and F7 (Kromasil, 250 × 4.6 mm, i.d. 5 μm, flow rate 0.7 mL/min, gradient mobile phase ACN–H_2O 20:80 in 11 min to 0:100 in 24 min; ELSD detection) and TLC of F6′ on a silica plate developed with CH_2Cl_2–MeOH, 97:3 and sprayed with a solution of phosphomolybdic acid.

dx.doi.org/10.1021/np400856h | J. Nat. Prod. 2014, 77, 1117–1122

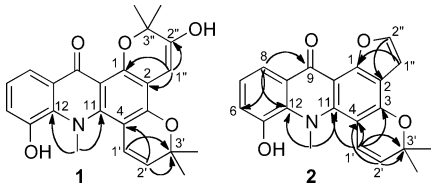

Figure 2. Selected HMBC correlations for compounds **1** and **2**.

Compound **2** was obtained as an amorphous powder. The HRESIMS showed an $[M + H]^+$ ion at m/z 348.1238, which in conjunction with the ^{13}C NMR spectroscopic data established the molecular formula of **2** as $C_{21}H_{18}NO_4$ (calcd 348.1236). The UV spectrum also revealed the existence of an acridone skeleton with absorption bands at 273 and 399 nm. The ^1H NMR data revealed the presence of a 2,2-dimethylpyran moiety, consisting of a set of doublets at δ_H 6.77 and 5.54, each with a 9.7 Hz coupling constant. These resonances were assigned to H-1′ and H-2′, respectively (Table 1). The *gem*-dimethyl group of the pyran ring resonated as a six-proton singlet at δ_H 1.53. The ^1H NMR spectrum also showed a set of doublets at δ_H 6.83 and 7.68 (H-1″ and H-2″, respectively), each with a coupling constant of 1.9 Hz, suggesting the presence of a furan ring. In addition, the ^1H NMR spectrum showed aromatic resonances for a 1,2,3-trisubstituted benzene ring as well as a resonance for an *N*-methyl group at δ_H 3.73. The HMBC correlations from H-1′ to C-3, C-4, and C-11 and from H-2′ to C-4 suggested that the 2,2-dimethylpyran moiety was attached to C-4 and C-3 (Figure 2). The HMBC correlations from H-1″ to C-1 and from H-2″ to C-2 established the location of the furan ring (Figure 2).

Compounds **1**−**4** were subjected to DYRK1A, CLK1, CDK1, CDK5, GSK3, and CK1 inhibition assays (Table 2). Acrifoline

Table 2. IC_{50}'s (in μM) of Compounds 1−4 against Various Kinases[a]

cpd	CDK1	CDK5	CLK1	DYRK1A	GSK3	CK1
1	>10	>10	>10	>10	>10	>10
2	>10	>10	7	5.7	>10	>10
3	>10	>10	≥10	2.2	>10	>10
4	5.3	9	0.17	0.075	2	>10
ref[b]	0.32	0.085	2.1	0.052	0.005	1.9

[a]Assays were carried out in duplicate. Specific activities for CDK1, CDK5, CK1, CLK1, DYRK1A, GSK-3 were respectively 60.1, 16.4, 28.9, 6.4, 29.4, and 35.4 pmol phosphate incorporated/μL kinase preparation/30 min. [b]6-Bromoindirubin-3′-monoxime.

(**4**) showed potent DYRK1A and CLK1 inhibition activities with IC_{50} values of 0.075 and 0.17 μM, respectively, whereas compounds **2** and **3** were less active, and chlorospermine A (**1**) was inactive. Despite the fact that no relevant structure−activity relationships could be established within this chemical series, it could be postulated that free hydroxy groups at C-1 and C-6 are critical for achieving inhibition of DYRK1A and CLK1. We next evaluated the selectivity of acrifoline (**4**) by determining its IC_{50} values on a panel of 14 kinases (Table 3 and Figure S3). Results revealed a modest selectivity with a preference toward DYRK1A. Acrifoline (**4**) and analogues thereof are currently being investigated in more detail in terms of its molecular, cellular, and animal model effects.

In order to better understand the influence of the substitution pattern of the acridone tricyclic system on their

Table 3. Selectivity of Acrifoline (4) in a Panel of 14 Purified Kinases[a]

kinase	IC_{50} (μM)
CDK1/cyclin B	1.1
CDK2/cyclin A	8.2
CDK5/p25	>10
CDK9/cyclin T	0.82
CK1δ/ε	8.7
CLK1	0.21
CLK2	0.68
CLK3	2.3
CLK4	0.22
DYRK1A	0.09
DYRK1B	0.35
DYRK2	1.7
DYRK3	1.2
GSK-3α/β	0.71

[a]Assays were carried out in duplicate.

specific binding to DYRK1A, we performed a molecular docking study of the compounds isolated into the DYRK1A ATP binding domain and compared the results obtained with the β-carboline alkaloid harmine. Molecular docking calculations (Figure 3A−D) provided more insight into the proposed structural details of the interaction between compounds **1**−**4** and the DYRK1A binding site. On the basis of molecular modeling, acrifoline (**4**) is proposed to interact with Glu203 and the conserved Lys188 through hydrogen bonds involving the C-6 hydroxy group and with the hinge region (backbone atoms of Glu239 and Leu241) through hydrogen bonds involving the C-1 hydroxy group. These interactions are similar to those observed in the crystal structure of the complex between harmine and DYRK1A (Figure 3E). Atalaphyllidine (**3**) is proposed to be positioned in a different way and forms hydrogen bonds between oxygen atoms at C-9, C-1, and C-5 and backbone atoms of Glu239, Leu241, and Ile165, respectively. Chlorospermine B (**2**) possesses yet another conformation, with hydrogen bonds between the C-5 hydroxy group and the side chains of Glu203 and Lys188. Finally, chlorospermine A (**1**) shows hydrogen bonds between oxygen atoms in positions C-5, C-9, and C-2″ and backbone NH of Leu241 and side chains of Asn244 and Asp307 (from the DFG motif), respectively. In addition, a possible $\pi-\pi$ stacking interaction between the "gatekeeper" residue Phe238 and compounds **2** and **4** might also contribute to their overall binding energy.

The predicted binding conformations of compounds **1**−**4** are strongly influenced by the substitution pattern of the acridone tricyclic system. For example, although no steric clashes prevent atalaphyllidine (**3**) from adopting the same conformation as acrifoline (**4**), its interaction with the DYRK1A binding site is driven by the presence of the C-5 hydroxy substituent, whereas the positioning of **4** is driven by the C-6 hydroxy substituent. Alternatively, chlorospermines A (**1**) and B (**2**) cannot adopt the same orientation as **4** because of steric clashes between the cyclic substituent at C-1/C-2 and the NCH_3 group and the side chains of Leu241 and Val173, respectively (Figure S2, Supporting Information).

The analysis of these molecular modeling results in light of the biological data (Table 2) suggests that strong, stabilizing interactions of the ligand with both conserved Lys188 and backbone atoms in the hinge region (Glu239 and/or Leu241)

dx.doi.org/10.1021/np400856h | J. Nat. Prod. 2014, 77, 1117−1122

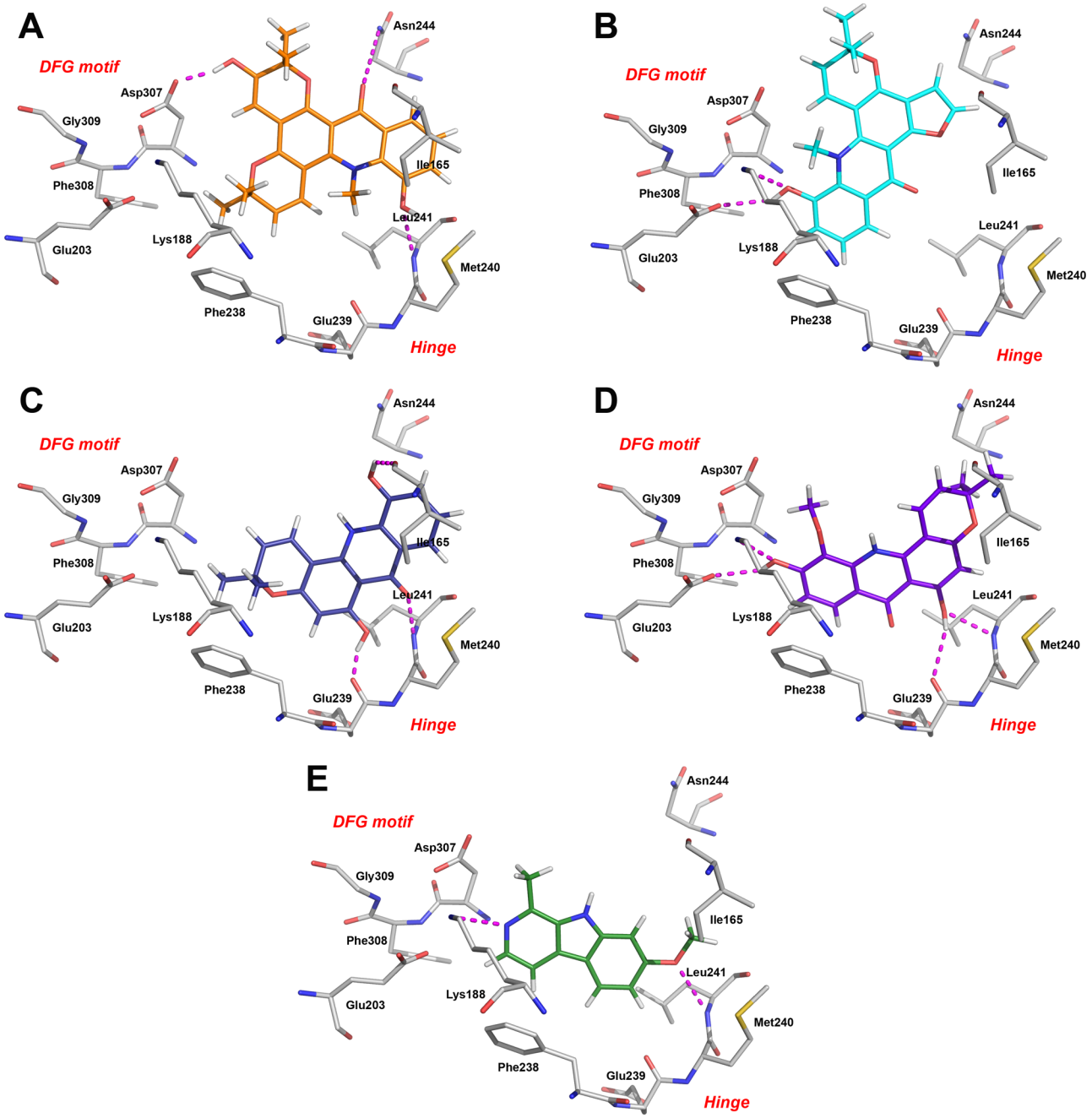

Figure 3. Docking conformations of compounds **1**–**4** (A–D) in the DYRK1A binding site. The conformation of harmine in the DYRK1A binding site (X-ray diffraction, PDB 3ANR) is shown for comparison (E).

are required for good biological activity (e.g., compound **4** and harmine, Figure 3D,E). When only one of these interactions is present, the strength of the protein–ligand interaction is predicted to be reduced (e.g., compounds **2** and **3**, Figure 3B,C). Compound **1** is predicted to interact mainly with the DFG motif, with the Asn244 residue, and to a lesser extent with the hinge region, which could explain the lack of biological activity determined experimentally for this compound (Table 2).

In conclusion, this is the first report of a natural acridone showing a potent DYRK1A-inhibiting activity. Molecular docking calculations provided structural details for the interaction between acrifoline (**4**), atalaphyllidine (**3**), chlorospermines A and B (**1** and **2**), and DYRK1A, which are in agreement with the biological data. Docking studies predict a binding mode for acrifoline (**4**), which showed the most potent DYRK1A-inhibiting activity, similar to that of harmine, a β-carboline alkaloid, and leucettines, currently considered the most potent bioavailable inhibitors of this enzyme.[14] Acridone could therefore represent a novel molecular scaffold in the search for new DYRK1A inhibitors.

EXPERIMENTAL SECTION

General Experimental Procedures. UV spectra were recorded on a PerkinElmer Lambda 5 spectrophotometer. IR spectra were recorded with a Nicolet FTIR 205 spectrophotometer. The NMR spectra were recorded on a Bruker 500 MHz instrument (Avance 500) for ^{1}H and 125 MHz for ^{13}C using $CDCl_3$ as solvent. HRESIMS was run on a Thermoquest TLM LCQ Deca ion-trap spectrometer.

dx.doi.org/10.1021/np400856h | J. Nat. Prod. 2014, 77, 1117–1122

Kromasil analytical and preparative C_{18} columns (250 × 4.6 mm and 250 × 21.2 mm; i.d. 5 μm, Thermo) were used for preparative HLPC separations using a Waters autopurification system equipped with a binary pump (Waters 2525), a UV−vis diode array detector (190−600 nm, Waters 2996), and a PL-ELS 1000 ELSD Polymer Laboratory detector. Silica gel 60 (6−35 μm) and analytical and preparative TLC plates (Si gel 60 F_{254}) were purchased from SDS (France). A C_{18} 140 g Versapack cartridge was used for flash chromatography using a Combiflash-Companion apparatus (Serlabo). All other chemicals and solvents were purchased from SDS (France).

Plant Material. *Glycosmis chlorosperma* was collected in Keluang, Johor Province, Malaysia, in July 2006. The plant was identified by T. Leong Eng, Botanist, University of Malaya. A voucher specimen (KL-5280) has been deposited at the Herbarium of the Department of Chemistry, Faculty of Science, University of Malaya, Kuala Lumpur, Malaysia.

Extraction and Isolation. The air-dried and powdered bark of *G. chlorosperma* (1 kg) was extracted with EtOAc (3 × 1 L, 1 h each, 38 °C, 100 bar), using a Zippertex static high-pressure, high-temperature extractor, developed in the ICSN Pilot Unit. The EtOAc crude extract was concentrated in a vacuum at 40 °C to yield 9.4 g of residue. This residue (8.9 g) was subjected to flash chromatography using a C_{18} 140 g Versapack cartridge with a gradient of MeCN−H_2O (20:80 to 100:0) at 20 mL/min to afford 12 fractions, F1−F12, according to their TLC profiles. Fraction F6 (788 mg, IC_{50} 0.23 μg/mL) was subjected to silica gel column chromatography (CC) using a gradient of CH_2Cl_2−MeOH (100:0−80:20) of increasing polarity, leading to 18 fractions (F1′−F18′) on the basis of TLC. Fraction F6′ (259 mg) was subjected to silica gel CC using a gradient of CH_2Cl_2−MeOH (100:0−80:20) to afford atalaphyllidine (**3**, 18.9 mg) and acrifoline (**4**, 6.7 mg). Fraction F10′ (16 mg) was subjected to preparative TLC using the system EtOAc−CH_2Cl_2 (90:10) to afford chlorospermine B (**2**, 2.5 mg). The purification of fraction F15′ (51 mg) using preparative TLC with the solvent system EtOAc−MeOH (98:2) afforded chlorospermine A (**1**, 3.5 mg).

*Chlorospermine A (**1**):* red, amorphous powder; UV (MeOH) λ_{max} (log ε) 275 (4.4) nm; IR ν_{max} 3210, 1595, 1665, 1178, 833 cm^{-1}; ^1H and ^{13}C NMR data, see Table 1; HRESIMS m/z $[M + H]^+$ 406.1656 (calcd for $C_{24}H_{24}NO_5$, 406.1654).

*Chlorospermine B (**2**):* red, amorphous powder; UV (MeOH) λ_{max} (log ε) 273 (4.2), 399 (3.4) nm; IR ν_{max} 3178, 1593, 1356, 1124, 833 cm^{-1}; ^1H and ^{13}C NMR data, see Table 1; HRESIMS m/z $[M + H]^+$ 348.1238 (calcd for $C_{21}H_{18}NO_4$, 348.1236).

Protein Kinase Assays. *Buffers.* Buffer A: 10 mM $MgCl_2$, 1 mM EGTA, 1 mM DTT, 25 mM Tris-HCl pH 7.5, 50 μg heparin/mL. Buffer C: 60 mM ß-glycerophosphate, 30 mM *p*-nitrophenylphosphate, 25 mM Mops (pH 7.2), 5 mM EGTA, 15 mM $MgCl_2$, 1 mM DTT, 0.1 mM sodium vanadate, 1 mM phenylphosphate.

Kinase Preparations and Assays. Native (CDK1, CK1, GSK-3) and recombinant (CDK5, CLK1, DYRK1A) kinases were purified by affinity chromatography. The active fractions were pooled, and catalytic activity of each preparation was tested in the presence of 15 μM cold ATP (final concentration) supplemented with radiolabeled ATP, using a range of volumes of each pooled fraction preparation. The objective of this test was (1) to determine the specific activity (listed in the legend of Table 2), (2) to ascertain that all further assays would be run under linear conditions (thereby allowing detection of linear inhibition), and (3) to ascertain that no more than 5−10% of the ATP substrate was consumed during the duration of the assay (30 min). As the inhibitors were most likely acting by competing at the ATP-binding site (as further supported by the modeling experiments reported in Figure 3), a standard 15 μM ATP concentration were used, which may not correspond to the optimal concentration for each enzyme. However, this allows a fast screening and unambiguous detection of ATP-competitive inhibitors. The IC_{50} values provided are thus relative values and should not be confused with K_i values, which are absolute values, independent of the ATP concentration. Kinase activities were assayed in buffer A or C, at 30 °C, at a final ATP concentration of 15 μM. Blank values were subtracted and activities expressed in % of the maximal activity, i.e., in the absence of inhibitors. Controls were performed with appropriate dilutions of DMSO. The GSK-3, CK1, DYRK1a, and CLK1 peptide substrates were obtained from Proteogenix (Oberhausbergen, France).

CDK1/cyclin B (M phase starfish oocytes, native) (0.1 μL active kinase preparation/assay) and CDK5/p25 (1 μL active kinase preparation/assay) were prepared as previously described.[15,16] Their kinase activity was assayed in buffer C, with 1 mg histone H1/mL, in the presence of 15 μM [γ-^{33}P] ATP (3000 Ci/mmol; 10 mCi/mL) in a final volume of 30 μL. After 30 min incubation at 30 °C, the reaction was stopped by harvesting onto P81 phosphocellulose papers (Whatman) using a FilterMate harvester (PerkinElmer), and the products were washed in 1% phosphoric acid. Scintillation fluid was added, and the radioactivity measured in a PerkinElmer counter. GSK-3$\alpha\beta$ (porcine brain, native) (1 μL active kinase preparation/assay) was assayed, as described for CDK1 but in buffer A and using a GSK-3-specific substrate (GS-1: YRRAAVPPSPSLSRHSSPHQSpEDEEE) (pS stands for phosphorylated serine).[17] Rat DYRK1A (vector kindly provided by Dr. W. Becker, Institute for Pharmacology and Toxicology, Aachen, Germany) (0.3 μL active kinase preparation/assay) was purified by affinity chromatography on glutathione-agarose and assayed in buffer A (+ 0.5 mg BSA/mL) using RS peptide (GRSRSRSRSRSR) (1 μg/assay) as a substrate.[18] CLK1 (mouse, recombinant, expressed in *E. coli* as GST fusion protein) (1.4 μL active kinase preparation/assay) was assayed in buffer A (+ 0.15 mg BSA/mL) with RS peptide (GRSRSRSRSRSR) (1 μg/assay). CK1δ/ε (porcine brain, native) (0.2 μL active kinase preparation/assay) was assayed in 3-fold-diluted buffer C, as described for CDK1 but using 25 μM CKS peptide (RRKHAAIGpSAYSITA), a CK1-specific substrate.[19]

Molecular Modeling. Sequence alignments were generated using ClustalX, version 2.0.[20] Molecular docking calculations were carried out using Gold 5.2,[21] with the Goldscore scoring function and the human DYRK1A protein structure (PDB code 3ANR[22]). Sequence alignment between the rat DYRK1A (used for the protein kinase assay) and the human DYRK1A (used for molecular docking) showed that there were only three mutations between these two proteins, in positions 32, 404, and 543 (Figure S1, see Supporting Information). Residue 404 is distant from the binding site (more than 43 Å), and the other two are toward the beginning and the end of the sequence, not present in the protein structure used for the docking, implying that the docking results can be reliably compared with the protein kinase assay data. The binding site was defined as a sphere with 15 Å radius around the CB atom of the "gatekeeper" Phe238 residue. Three-dimensional coordinates of the ligands were obtained using Corina, version 3.44 (http://www.molecular-networks.com/). Images were generated using PyMol version 1.6 (http://www.schrodinger.com/).

■ ASSOCIATED CONTENT

Ⓢ Supporting Information

NMR spectra for compounds **1** and **2**, sequence alignment for rat and human DYRK1A, kinase activity data (**4**), and superimposition of compounds **1**−**4** in the DYRK1A binding site are available free of charge via the Internet at http://pubs.acs.org.

■ AUTHOR INFORMATION

Corresponding Author

*E-mail: marc.litaudon@cnrs.fr. Tel: + 33 1 69 82 30 85. Fax: + 33 1 69 07 72 47.

Notes

The authors declare no competing financial interest.

■ ACKNOWLEDGMENTS

We are very grateful to Prof. D. Crich (Wayne State University) for the fellowship (M.A.B.). This research was supported by grants from University Malaya (UM-MOHE UM.C/625/1/HIR/MOHE/SC/37), the Fonds Unique Interministériel

(FUI) PHARMASEA project, the European Union 7th Framework Program (FP7) Micro-Therapy project, the European Union 7th Framework Program Knowledge-Based Bio-economy (FP7-KBBE)-BlueGenics 2012 grant, the Association France-Alzheimer (Finistère), the Centre Régional d'Innovation et de Transfert de Technologie (CRITT)-Santé Bretagne, and Fondation Jérôme Lejeune. This work has also benefitted from an "Investissement d'Avenir" grant managed by Agence Nationale de la Recherche (CEBA, ref. ANR-10-LABX-25-01).

REFERENCES

(1) Liu, J.; Hu, Y.; Waller, D. L.; Wang, J.; Liu, Q. *Nat. Prod. Rep.* **2012**, *29*, 392−403.
(2) Becker, W.; Sippl, W. *FEBS J.* **2011**, *278*, 246−256.
(3) (a) Marti, G.; Eparvier, V.; Morleo, B.; Ven, J.; Apel, C.; Bodo, B.; Amand, S.; Dumontet, V.; Lozach, O.; Meijer, L.; Guéritte, F.; Litaudon, M. *Molecules* **2013**, *18*, 3018−3027. (b) Apel, C.; Dumontet, V.; Lozach, O.; Meijer, L.; Guéritte, F.; Litaudon, M. *Phytochem. Lett.* **2012**, *5*, 814−818.
(4) Sprengel, K. *Syst. Vegetabilium* **1827**, *4*, 162.
(5) Whitmore, T. C. In *Tree Flora of Malaya; A Manual for the Forester*; Whitmore, T. C., Ed.; Longman: Hong Kong, 1972; Vol. *1*, pp 380−382.
(6) (a) Wang, J.; Yang, X.; Di, Y.; Wang, Y.; Shen, Y.; Hao, X. *J. Nat. Prod.* **2006**, *69*, 778−782. (b) Lukaseder, B.; Vajrodaya, S.; Hehenberger, T.; Seger, C.; Nagl, M.; Lutz-Kutschera, G.; Robien, W.; Greger, H.; Hofer, O. *Phytochemistry* **2009**, *70*, 1030−1037.
(7) (a) Yahayu, M. A.; Rahmani, M.; Hashim, N. M.; Amin, M. A. M.; Ee, G. C. L.; Sukari, M. A.; Akim, A. M. *Molecules* **2011**, *16*, 4401−4407. (b) Wu, T.-S.; Furukawa, H.; Kuoh, C.-S.; Hsu, K.-S. *J. Chem. Soc., Perkin Trans. 1* **1983**, 1681−1688. (c) Quader, M. A.; Nutan, M. T. H.; Rashid, M. A. *Fitoterapia* **1999**, *70*, 305−307. (d) Ono, T.; Ito, C.; Furukawa, H.; Wu, T.-S.; Kuoh, C.-S.; Hsu, K.-S. *J. Nat. Prod.* **1995**, *58*, 1629−1631.
(8) (a) Yang, G.-Z.; Wu, Y.; Chen, Y. *Helv. Chim. Acta* **2012**, *95*, 1449−1454. (b) Ito, C.; Itoigawa, M.; Sato, A.; Hasan, C. M.; Rashid, M. A.; Tokuda, H.; Mukainaka, T.; Nishino, H.; Furukawa, H. *J. Nat. Prod.* **2004**, *67*, 1488−1491. (c) Bhattacharyya, P.; Chowdhury, B. K. *J. Nat. Prod.* **1985**, *48*, 465−466.
(9) Bhattacharyya, P.; Chowdhury, B. K. *Phytochemistry* **1985**, *24*, 634−635.
(10) Sarkar, M.; Chakraborty, D. P. *Phytochemistry* **1977**, *16*, 2007−2008.
(11) (a) Hofer, O.; Greger, H.; Lukaseder, B.; Vajrodaya, S.; Bacher, M. *Phytochemistry* **2000**, *54*, 207−213. (b) Greger, H.; Zechner, G.; Hofer, O.; Vajrodaya, S. *J. Nat. Prod.* **1996**, *59*, 1163−1168. (c) Greger, H.; Zechner, G.; Hofer, O.; Hadacek, F.; Wurz, G. *Phytochemistry* **1993**, *34*, 175−179. (d) Greger, H.; Hadacek, F.; Hofer, O.; Wurz, G.; Zechner, G. *Phytochemistry* **1993**, *32*, 933−936.
(12) Basa, S. C. *Experientia* **1975**, *31*, 1387.
(13) Brown, R.; Lahey, F. *Aust. J. Chem.* **1950**, *3*, 593−614.
(14) (a) Göckler, N.; Jofre, G.; Papadopoulos, C.; Soppa, U.; Tejedor, F. J.; Becker, W. *FEBS J.* **2009**, *276*, 6324−6337. (b) Tahtouh, T.; Elkins, J. M.; Filippakopoulos, P.; Soundararajan, M.; Burgy, G.; Durieu, E.; Cochet, C.; Schmid, R. S.; Lo, D. C.; Delhommel, F.; Oberholzer, A. E.; Pearl, L. H.; Carreaux, F.; Bazureau, J. P.; Knapp, S.; Meijer, L. *J. Med. Chem.* **2012**, *55*, 9312−9330. (c) Debdab, M.; Renault, S.; Soundararajan, M.; Fedorov, O.; Filippakopoulos, P.; Lozach, O.; Babault, L.; Tahtouh, T.; Baratte, B.; Ogawa, Y.; Hagiwara, M.; Eisenreich, A.; Rauch, U.; Knapp, S.; Meijer, L.; Bazureau, J.-P. *J. Med. Chem.* **2011**, *54*, 4172−4186.
(15) Leclerc, S.; Garnier, M.; Hoessel, R.; Marko, D.; Gretchen, B.; Snyder, P.; Greengard, P.; Biernat, J.; Wu, Y.-Z.; Mandelkow, E.-M.; Eisenbrand, G.; Meijer, L. *J. Biol. Chem.* **2001**, *276*, 251−260.
(16) Bach, S.; Knockaert, M.; Reinhardt, J.; Lozach, O.; Schmitt, S.; Baratte, B.; Koken, M.; Coburn, S. P.; Tang, L.; Jiang, T.; Liang, D. C.; Galons, H.; Dierick, J. F.; Pina, L. A.; Meggio, F.; Totzke, F.; Schachtele, C.; Lerman, A. S.; Carnero, A.; Wan, Y.; Gray, N.; Meijer, L. *J. Biol. Chem.* **2005**, *280*, 31208−31219.
(17) Primot, A.; Baratte, B.; Gompel, M.; Borgne, A.; Liabeuf, S.; Romette, J. L.; Costantini, F.; Meijer, L. *Protein Expr. Purif.* **2000**, *20*, 394−404.
(18) Beauchard, A.; Ferandin, Y.; Frère, S.; Lozach, O.; Blairvacq, M.; Meijer, L.; Thiéry, V.; Besson, T. *Bioorg. Med. Chem.* **2006**, *14*, 6434−6443.
(19) Reinhardt, J.; Ferandin, Y.; Meijer, L. *Protein Expr. Purif.* **2007**, *54*, 101−109.
(20) Larkin, M. A.; Blackshields, G.; Brown, N. P.; Chenna, R.; McGettigan, P. A.; McWilliam, H.; Valentin, F.; Wallace, I. M.; Wilm, A.; Lopez, R.; Thompson, J. D.; Gibson, T. J.; Higgins, D. G. *Bioinformatics* **2007**, *23*, 2947−2948.
(21) Verdonk, M. L.; Cole, J. C.; Hartshorn, M. J.; Murray, C. W.; Taylor, R. D. *Proteins* **2003**, *52*, 609−623.
(22) Ogawa, Y.; Nonaka, Y.; Goto, T.; Ohnishi, E.; Hiramatsu, T.; Kii, I.; Yoshida, M.; Ikura, T.; Onogi, H.; Shibuya, H.; Hosoya, T.; Ito, N.; Hagiwara, M. *Nat. Commun.* **2010**, *1*, 1−9.

NOTE ADDED AFTER ASAP PUBLICATION

This paper was published ASAP on May 5, 2014, with incorrect graphics in Figures 1 and 3. The corrected version reposted on May 6, 2014.